Evaluation of Corrosion Inhibition of Carbon Steel in 1M HCl medium by essential oil of seed *Carum Carvi*

L. El Hattabi[a], M. EL Moudane[a], H. Harhar[b], A. Bellaouchou[a], A. Ghanimi[a], A. Guenbour[a], J. Costa[c], J. M. Desjobert[c] and M. Tabyaoui[a]*

[a] *Laboratory of Nanotechnology, Materials and Environment, Department of Chemistry, Faculty of Science, University Mohammed V, Av. Ibn Batouta, BP. 1014 Rabat, Morocco*
[b]*Laboratoire de Chimie des Plantes et de Synthèse Organique et Bioorganique, Faculté des Sciences, Université Mohammed V, Rabat, Morocco.*
[c]*Laboratoire de Chimie des Produits Naturels, Faculté des Sciences et techniques, Université de Corse, UMR CNRS 6134, Corse, France*

Abstract

The inhibiting effect of essential oil of *Carum Carvi* (Carum.C) on the corrosion of carbon steel in 1M HCl solution has been investigated by different techniques such as weight loss, potentiodynamic polarization and electrochemical impedance (EIS) methods at different concentrations of inhibitor ranging from 0,6 to 3 g/L. Essential oil from *Carum Carvi* was obtained by Clevenger-type water distillation. The essential oil was identified by gas chromatography-mass Spectrometry (GC and GC/MS). The major compounds identified are: Carvone (67.3 %) and Limonene (28.8 %). The results of polarization show that the inhibition efficiency increases with increasing the Carum.C oil concentration to attain a maximum value of 92 % at 3 g/L. The Nyquist plots showed also that increasing oil concentration, charge-transfer resistance increased and double-layer capacitance decreased, involving increased inhibition efficiency. The study of the effect of the temperature (303 - 343 K) on the behavior of the carbon steel in 1M HCl medium with and without inhibitor reveals that the inhibition efficiencies decreases slightly with temperature increasing. Carum.C oil is adsorbed on the steel surface according the Langmuir isotherm model. The parameters (E_a^*, ΔG_a^*, ΔH_a^* and Kads) were estimated and discussed. Physical adsorption is proposed for the corrosion inhibition mechanism and the process followed the kinetic/thermodynamic model of El-Awady et al. in the temperature range from 303 to 343 K.

Keywords: Essential oil, Steel, EIS, Inhibitor, Gravimetry, *Carum Carvi*

1. Introduction

Corrosion is a huge problem for materials in different domains mechanical, civil and petrochemical engineering. Metallic materials are often in contact with a liquid or gaseous aggressive environment; therefore the corrosion phenomenon is a surface problem or more precisely the interface between a metal and an aggressive environment. The corrosion process leads to deterioration of metallic materials. Corrosion problems are generally related to operating and equipment's maintenance problems, leading to discontinuation of partial and even total recurring process, resulting in severe economic losses [1]. Carbon steel is the main construction material, which is widely used in most major industries especially in food, petroleum, and power generation, chemical and electrochemical industries. The use of inhibitors to protect carbon steel against the destructive acidic attack is effective and widely used in many industries [2;3]. Recently, the inhibition of steel corrosion in acidic solutions by different types of organic inhibitors has been studied extensively [4-8]. Acidic solutions are generally used in many industrial

J. Mater. Environ. Sci. 7 (9) (2016) 3162-3178 ISSN : 2028-2508 CODEN: JMESCN

EL Hattabi et al.

processes for removing scale and undesirable rust. Hydrochloric and sulfuric acids are widely used in metal pickling processes. The use of inhibitors is one of the most convenient methods for the protection against corrosion, in particular acid medium [9 -12]. Recently, several studies have been conducted on the inhibition of metals corrosion by the plant extracts [13-19], and essential oils [20;21].

The cited oils include: Chamomile oil [22], pennyroyal oil [23], eucalyptus oil, [24] jojoba oil [25], rosemary oil [26-27], Artemisia Oil [28-30], lavender oil [31], Menthol derivatives [32], eugenol and acetyleugenol [33], Pulegone [34] and limonene [35]; these oils are found very effective in acidic environments.

The objective of this study was to investigate the inhibitory effects of *Carvi Carum* oil as a corrosion inhibitor for carbon steel in a 1M HCl medium of hydrochloric acid. Weight loss measurements, potentiodynamic polarization curves and electrochemical impedance measurements were used.

2. Experimental

2.1. Plant material and hydrodistillation
The seeds of *Carum Carvi* (Carum.C) were collected from the Agouray region (Morocco) in June, 2013; they are dried in the shade and stored in the laboratory at room temperature (298 K). They were then ground to a fine powder. The seeds of Carum.C were affected by hydrodistillation (Clevenger) for 4h [36].

2.2. Gas chromatography–mass spectrometry (GC-MS)
Samples were analyzed with a Perkin-Elmer turbo mass detector (quadrupole) coupled to a Perkin-Elmer Autosystem XL equipped with the fused-silica capillary columns Rtx-1 and Rtx-wax. Carrier gas: helium (1 mL/min), ion source temperature: 150 °C, oven temperature programmed from 60 °C to 230 °C at 2 °C/min and then held isothermally at 230 °C (35 min), injector temperature: 280 °C, energy ionization: 70 eV, electron ionization mass spectra were acquired over the mass range 35– 350 Da, split: 1/80, injection volume: 0.2 μL of pure oil.

2.3. Components identification
The identification of the essential oil constituents was based on: (i) comparison with the mass spectra of authentic reference compounds where possible and by reference to WILEY275,NIST 02 and Adams mass spectral libraries [37-40] (ii) comparison of their retention index (RI), calculated relative to the retention times of a series of C-5 to C-30 n-alkanes, with linear interpolation, with those of our own library of authentic compounds or literature data [40,41].

2.4. Electrolytes and electrodes:
In order to study the inhibitive action of essential oil of Carum.C towards the corrosion of carbon steel (C38) in acid solution, corrosion tests were performed in the aggressive solutions of 1M/HCl were prepared by dilution of analytical grade 37% HCl in distilled water. We studied the effect of temperature on the inhibition efficiencies without or with different concentrations of inhibitor; all the tests were carried out in the temperature range 303– 343 K. The solution tests are freshly prepared before each experiment by adding the oil directly to the corrosive solution. The range concentration of employed Carum.C oil was varied from 0.6 to 3 g/L and the solution in the absence of Carum.C oil was taken as blank for comparison. The composition of the carbon steel used in experimental was: 0.38% C, 0.23% Si, 0.68% Mn, 0.077% Cr, 0.016% S, 0.16% Cu, 0.011% Ti, 0.052% Ni, 0.009% CO. Specimens which were used in the weight loss experiment were coupons with dimensions 1 x 3.3 x 0.3 cm and surface used in the electrochemical experiments is 1 cm^2. Prior to all measurements, the C38 specimens were abraded with a series of emery papers SiC (120, 600 and 1200), then washed with distilled water, acetone and dried.

2.5. Corrosion tests
2.5.1 Weight loss method:
Weight loss measurements were carried out in a double walled glass cell equipped with a thermostat-cooling condenser. The solution volume was 50 ml. The used steel specimens had a rectangular form (0.3 cm x 1cm x 3.3

cm). The immersion time for the weight loss measurements were carried out at the definite time interval of 6 hours using an analytical balance (precision ± 0.1 mg) in the temperature range 303-343 K. After six hours the specimens were removed, washed with distilled water, dried and reweighed to determine the overall weight loss. The percentage inhibition efficiency (IE %) was calculated from equation (1): [42;43]

$$IE\,(\%) = \frac{W_1 - W_2}{W1}\,X\,100 \qquad (1)$$

Where W_1 and W_2 are weight losses of steel in uninhibited and inhibited solutions, respectively. Weight loss allowed us to calculate the mean corrosion rate as expressed in mg cm^{-2}h^{-1}.

2.5.2 Electrochemical measurements
The electrochemical study was carried out using a potentiostat PGZ301 controlled by a PC supported by Volta master 4 software. A conventional three-electrode cylindrical Pyrex glass cell was used. The temperature was thermostatically controlled. The saturated calomel electrode (SCE) and platinum electrode were used as reference and auxiliary electrodes respectively. The working electrode is in the form of a rectangular from carbon steel of the surface 1 cm^2.

2.5.3 Potentiodynamic polarization
Anodic and cathodic potentiodynamic polarization curves were plotted separately at a polarization scan rate of 1mV/s started from an initial potential of -800 to -300 mV/SCE. Before all experiments, the potential was stabilized at free potential during 60 min to establish a steady state open circuit potential (Eocp). After measuring the Eocp, the electrochemical measurements were performed. Corrosion current densities were obtained from the polarization curves by linear extrapolation of the Tafel curves.

2.5.4 Electrochemical impedance spectroscopy (EIS):
The Electrochemical impedance spectroscopy (EIS) experiments were conducted in the frequency between 100 kHz and 10 mHz at open circuit potential, with 10 points per decade, at the resting potential, after 60 min of acid immersion, by applying 10 mV ac voltage peak-to-peak. The impedance diagrams are given in the Nyquist representation. The percentage inhibition efficiency (IE) was calculated from the following equation [44]:

$$IE\,(\%) = \frac{R_2 - R_1}{R_2} * 100 \quad (2)$$

Where IE% inhibitory efficiency; R_1 and R_2 are charge transfer resistance of steel in uninhibited and inhibited solutions, respectively.

3. Results and discussion
3.1. Analysis of the essential oil
From the GC/MS analysis of essential oil, more than 98.1% of total compounds were identified (Table 1). The retention time of volatile compounds (Ira and Irp) and their percentage are summarized in Table 1. The major components were Limonene (28.8 %) and Carvone (67.3 %).

3.2. Weight loss measurements: effect of plant oil concentration and temperature
The effect of addition of essential oil (E oil) of *Carum Carvi* seeds tested at different concentrations on the corrosion of carbon steel in 1 M HCl solution was studied by weight loss measurements after 6 h of immersion period. Fig. 1 and Fig. 2 shows the corrosion rate (W) and inhibition efficiency (IE%) of carbon steel exposed to 1M HCl at 303, 313, 323, 333 and 343 K in the absence and the presence of various concentrations of inhibitor. From these figures we can observe at the same temperature, that the value of inhibition efficiency increases while corrosion rate decreases with increase of inhibitor concentrations. We noted that essential oil used in this study showed excellent corrosion inhibitor for carbon steel in 1 M HCl at 303 K, especially for strong concentration (73 % for 3 g/L).This effect could expressed by the adsorption of active compounds existing in the oil on the carbon steel surface, which leads to a decrease of the surface area offered for corrosion.

Table 1: Chemical composition of *Carum Carvi* essential oil from Morocco.

N°	Composés	Ir apol	Ir pol	HE% apol	Ir Lit
1	Myrcene	981	1158	0.3	987
2	Limonene	1024	1202	28.8	1025
3	Camphor	1121	1512	0.2	1123
4	Z-dihydro Carvone	1171	1591	0.2	1172
5	Estragole	1175	1657	0.2	1175
6	E-dihydro Carvone	1178	1615	0.2	1177
7	cis-Carveol	1206	1848	0.4	1210
8	Carvone	1223	1722	67.3	1214
9	Peryllaldehyde	1247	1766	0.3	1260
10	Thymol	1262	2191	0.2	1267
TOTAL		**98.1**			

Ir apol = retention indices on the apolar column (Rtx-1)
Ir pol = retention indices on the polar column (Rtx-Wax)
HE%= Relative percentages of components (%) are calculated on GC peak areas on the apolar column
Ir lit = retention indices on the apolar column of literature

Carvone (67.3 %)   Limonene (28.8 %)
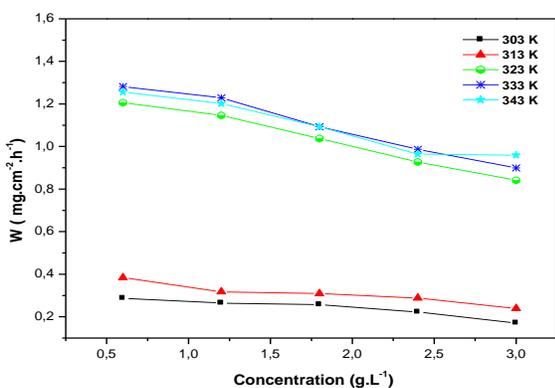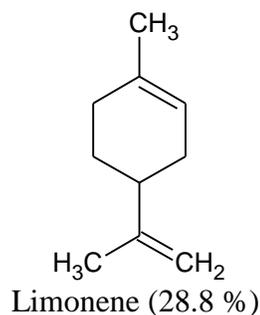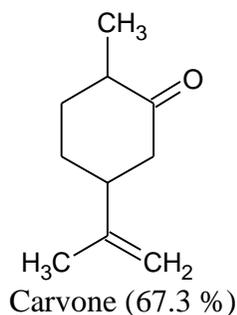
Figure 1: Corrosion rate of C-steel in 37% HCl with and without essential oil at 30, 40, 50, 60 and 70°C
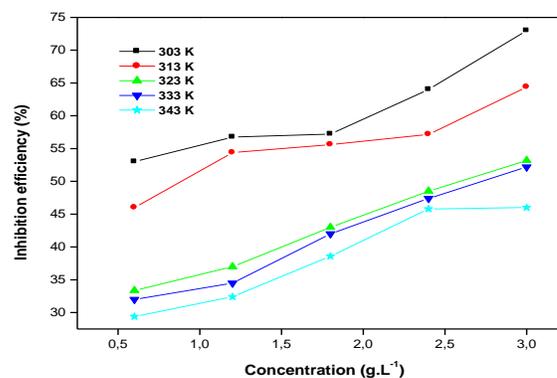
Figure 2: Inhibition efficiency plots of mild steel in 37% HCl with essential oil at 30, 40, 50, 60 and 70°C

Table 2: Effect of temperature on the corrosion rate and inhibition efficiency for the corrosion of C-steel in 1M HCl medium

Temperature (K)	C(g/l)	E %	$W(mg.cm^{-2}.h^{-1})$
303	Blank	_	0.610
	0.6	53.00	0.287
	1.2	56.75	0.264
	1.8	57.22	0.257
	2.4	64.00	0.222
	3	73 .00	0.171
313	Blank	_	0.712
	0.6	46.02	0.384
	1.2	54.38	0.317
	1.8	55.60	0.309
	2.4	57.17	0.288
	3	64.39	0.239
323	Blank	_	1.809
	0.6	33.36	1.206
	1.2	37.00	1.146
	1.8	43.00	1.037
	2.4	48.51	0.927
	3	53.18	0.841
333	Blank	_	1.879
	0.6	32.00	1.282
	1.2	34.50	1.229
	1.8	42.00	1.093
	2.4	47.40	0.987
	3	52.20	0.899
343	Blank	_	1.78
	0.6	29.40	1.256
	1.2	32.40	1.202
	1.8	38.60	1.093
	2.4	45.80	0.964
	3	46.00	0.959

Examination of Table 2 revealed that an increase in temperature increases corrosion rate values, while the addition of oil decreases the IE% values proportionally with temperature. This can be explained by the decrease of the strength of adsorption processes at elevated temperature and suggested a physical adsorption mode.

3.3. Potentiodynamic polarization

The potentiodynamic polarization curves of *Carum.C* E oil performed in 1M HCl in the absence and the presence of different concentrations of E oil at 303 K is presented in Figure 3. The values of electrochemical parameters associated with polarization measurements, such as corrosion potential (Ecorr), corrosion currents densities (Icorr), anodic slop (βa) and cathodic Tafel slope (βc) are listed in Table 3.The percentage of inhibition efficiency IE (%) and surface coverage (θ) were calculated using the following formulas:

$$IE = \frac{i_0 - i_1}{i_0} \times 100 \qquad (3)$$

$$\theta = \frac{i_0 - i_1}{i_0} \qquad (4)$$

Where i_0 and i_1 are respectively the corrosion current densities without and with inhibitor, determined by extrapolation of cathodic Tafel lines to the corrosion potential. In linear polarization method, the polarisation resistance Rp, was calculated from the Stern–Geary equation [45]

$$i_{corr} = \frac{\beta a\ \beta c}{2,303\,(\beta a + \beta c) Rp} \qquad (5)$$
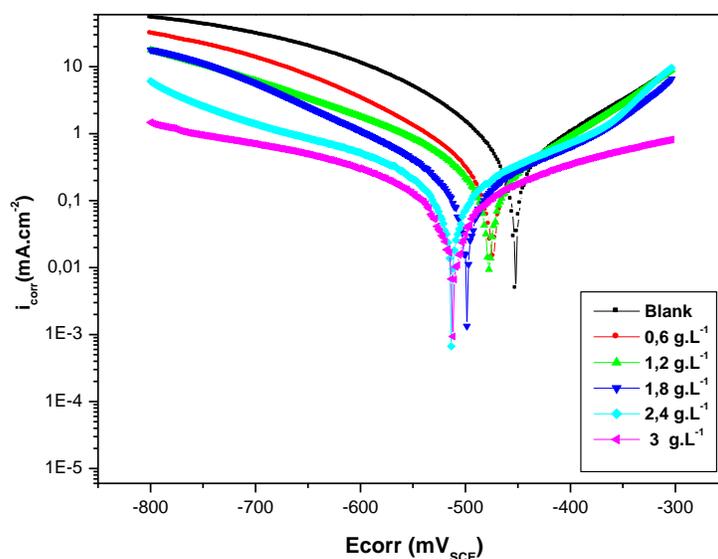
Figure 3: Polarization curves of steel in 1M/HCl without and with various concentrations of EO at 303 K.

It's obvious from electrochemical polarization measurements, that the concentration of inhibitors increase the inhibition efficiency and surface coverage degrees, while current densities decreases and the potential current moving to negative values (Tables 3). According to these data, these compounds are cathodic inhibitors and are adsorbed on the steel. This decrease of the current can be explained by the inhibitory action of this inhibitor. The anodic Tafel slope (βa) and the cathodic Tafel slope (βc) of *Carum.C* changed with inhibitor concentration. This observation suggests that the inhibitor molecules controlled the two reactions and adsorbed on the metal surface by blocking the active sites on the metal surface, retarding the corrosion reaction. The inhibition efficiency (IE %) increases with inhibitor concentration reaching 91.6 % at 3 g/L. These results suggest that the inhibitory action depends on the potential of corrosion and a desorption process appears at high potential [46]. These findings are suggesting that the *Carum.C* E oil is a type cathodic inhibitor for the corrosion of C38 in 1 M HCl.

Table 2: Polarization parameters and IE% for carbon steel corrosion in 1M HCl without and with various concentrations of *Carum.C* E oil at 303 K

Inhibitor	Concentration $(g.L^{-1})$	Ecorr (mV_{SCE})	Icorr $(\mu A.cm^{-2})$	βa (mV/dec)	-βc (mV/dec)	E%	θ
Blank	--	-451.6	144.71	164.7	112.9	--	--
E.O	0.6	-474.5	32.14	150.5	120.4	77.8	0.778
	1.2	-477.5	26.93	128.6	141.1	81.4	0.814
	1.8	-498.2	24.66	186.9	137.9	83.0	0.830
	2.4	-426.9	22.69	137.8	131.9	84.3	0.843
	3	-512.3	12.09	198.7	183.3	91.6	0.916

3.4. Electrochemical impedance spectroscopy results.

The corrosion behavior of carbon steel in 1M HCl medium with and without inhibitor is also investigated by the electrochemical impedance spectroscopy (EIS) at 303 K after 60 min of immersion. The charge-transfer resistance (Rt) values are calculated from the difference in impedance at lower and higher frequencies, as suggested by Tsuru and al [47]. The double-layer capacitance (C_{dl}) and the frequency at which the imaginary component of the impedance is maximal ($-Z_{max}$) are found as represented in the following equation:

$$C_{dl} = \frac{1}{2\pi f_{max} \ R_{ct}} \qquad (6)$$

Where f_{max} is the frequency at which the imaginary component of the impedance (Z_{im}) is maximum and Rt is the diameter of the loop .Table 4. Gives values of charge-transfer resistance R_{ct} , double-layer capacitance C_{dl}, and f_{max} derived from Nyquist plots and inhibition efficiency.

Table 3: Impedance data of carbon steel (C_{38}) in 1 M HCl without and with different concentrations of Carum.C E oil at 303 K

Inhibitor	C $(g .L^{-1})$	R_s $(\Omega.cm^{2})$	R_{ct} $(\Omega.cm^{2})$	f_{max} (Hz)	C_{dl} $(\mu F.cm^{-2})$	*IE* (%)
E oil 1 M HCl *Carum Carvi*	Blank	1.559	23.81	158.23	40.28	--
	0.6	1.501	113.30	100.00	33.21	79.0
	1.2	1.336	143.70	158	23.79	83.4
	1.8	1.546	164.60	40.000	18.40	85.5
	2.4	1.670	176.00	40.000	25.23	86.5
	3	3.194	198.50	40.000	18.85	88.0

Inhibitor can be associated with a decrease in capacitance of the metal. According to Helmholtz model [48]:

$$C_{dl} = \frac{\varepsilon°\varepsilon}{d} A \qquad (7)$$

Where $\varepsilon°$ is the air permittivity, ε is the local dielectric constant, the thickness of the film and A is the surface area of the electrode. while the decrease in C_{dl} is likely due to a decrease in the local dielectric constant and/or an increase in the thickness of a protective layer at the electrode surface, which would therefore enhance the corrosion resistance of the studied C38 in 1M HCl medium [49].

The significant difference between the inhibition efficiencies determined by weight loss and electrochemical measurements (tables 2,3 and 4) may be related to lack of stirring during analyzes weight loss thing which increases the insolubility problem of our oil in the 1M HCl medium.

The Nyquist plots for steel in 1M HCl medium in the absence and presence of different Carum.C oil concentrations are shown in Fig 4. These plots indicate that the dissolution process occurs under activation control. The impedance response consisted of characteristic semicircles. These semicircles are of a capacitive type whose size increases with increasing concentrations up to 3 g/L.
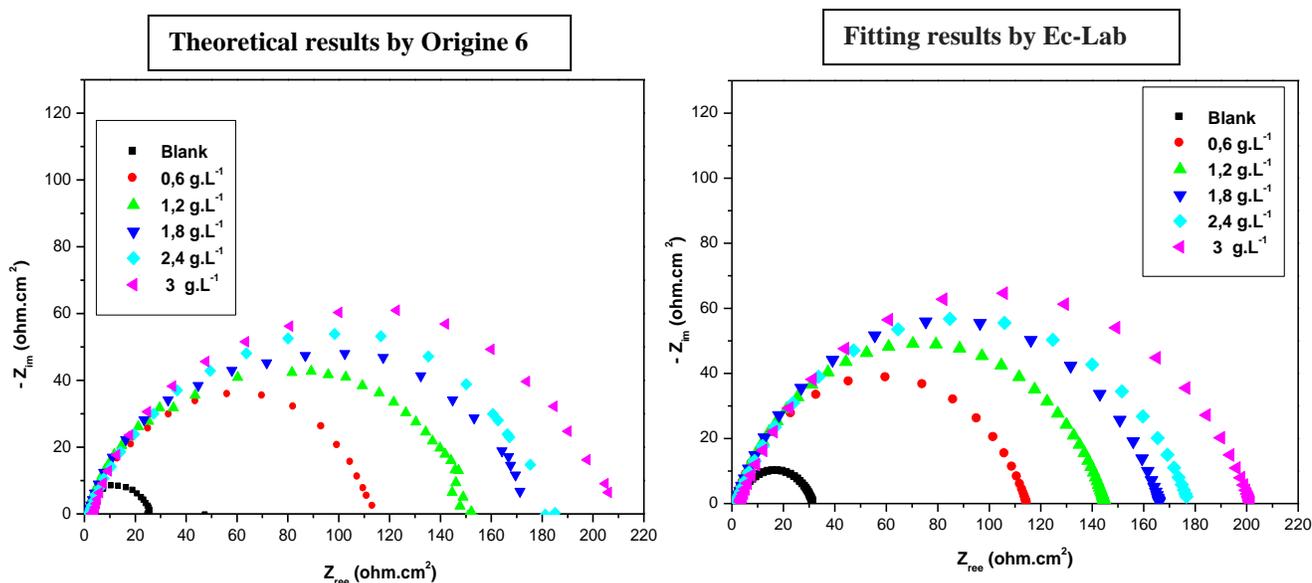
Figure 4: Nyquist plots of the corrosion of oil Carum.C in 1M HCl medium without and with different concentrations of E oil at 303 K

The data indicate that increasing charge transfer resistance is associated with a decrease in the double layer capacitance up to a critical concentration (3 g/L). The decrease in the C_{dl} values could be attributed to the adsorption of the chemical constituents of Carum.C E oil at the metal surface. It has been reported that the adsorption process on the metal surface is characterized by a decrease in C_{dl} [50]

The impedance spectra for different Nyquist plots were analyzed by fitting the experimental data to a simple equivalent circuit model (Fig. 5) which includes the solution resistance Rs and the double layer capacitance (C_{dl}) which is placed in parallel to charge transfer resistance element, Rct.
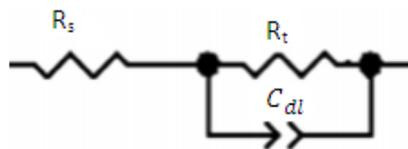
Figure 5: Equivalent circuit for impedance analysis

The C_{dl} were calculated from impedance measurements using the relation 6, the values of % inh are in quite good agreement with the results obtained previously from polarization measurements (Table 3). This demonstrates the fact that the corrosion rate depends on the chemical nature of the electrolyte and the temperature of the medium, rather than the applied technique.

A lot of natural products were previously used as corrosion inhibitors in various acidic media and their optimum concentrations were reported. For examples, The highest inhibition efficiency exhibited by the aqueous extract of the leaves of henna (*Lawsonia*) for C–steel corrosion in 1M HCl solutions was 95.78% with additives concentration of 800 ppm at 30°C [51]. These data and our results for the corrosion of steel in 1 M HCl acid in

presence of different plant extracts suggests that the oil essential (EO) could serve as effective corrosion inhibitors.

3.5. Effect of temperature and activation energy

To assess the influence of temperature on corrosion and corrosion inhibition processes, polarization tests were carried out at various temperatures (303–343 K) in the absence and presence of various concentrations of Carum.C E oil, as shown in Figures 6,7,8,9,10 and 11.
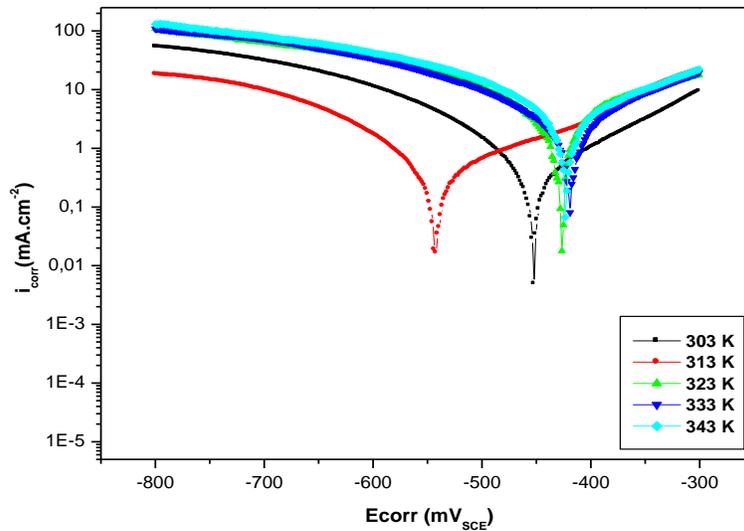
Figure 6: Potentiodynamic polarization curves for steel in 1M HCl at various temperatures in the absence of inhibitor.
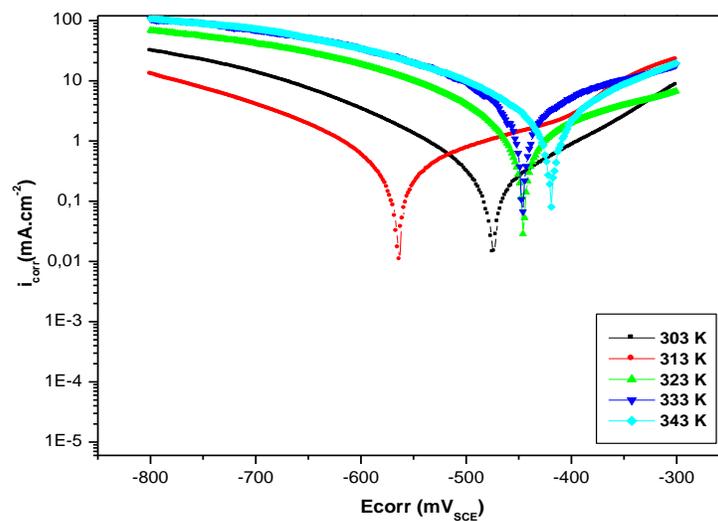
Figure 7: Potentiodynamic polarization curves for steel in 1M HCl at various temperatures for concentration 0.6 g/L the E oil inhibitor
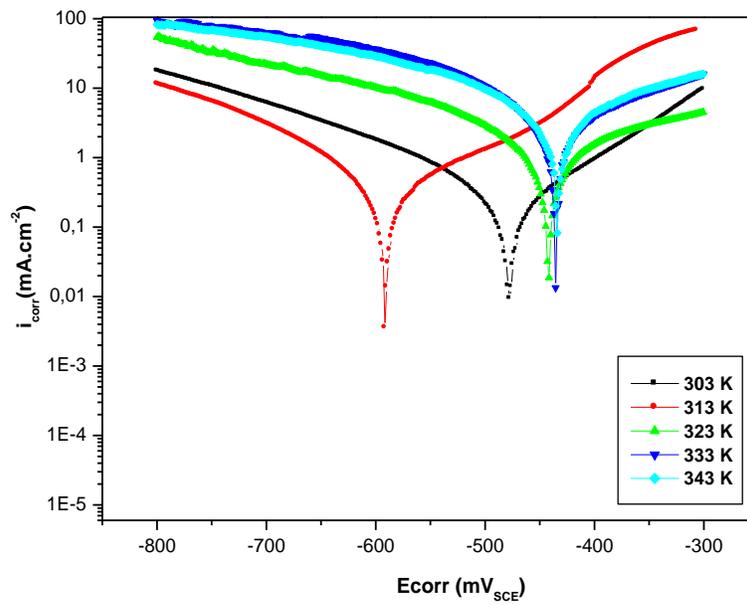
Figure 8: Potentiodynamic polarization curves for steel in 1M HCl at various temperatures for concentration 1.2 g/L the E oil inhibitor.
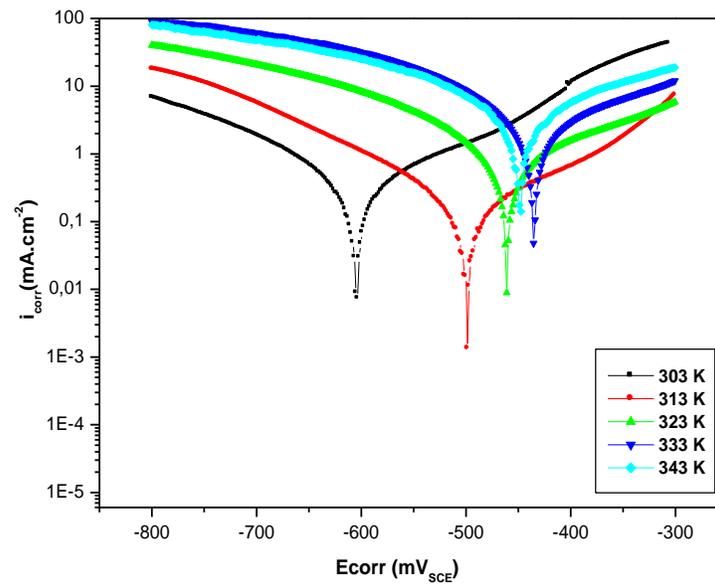
Figure 9: Potentiodynamic polarization curves for steel in 1M HCl at various temperatures for concentration 1.8 g/L the E oil inhibitor.
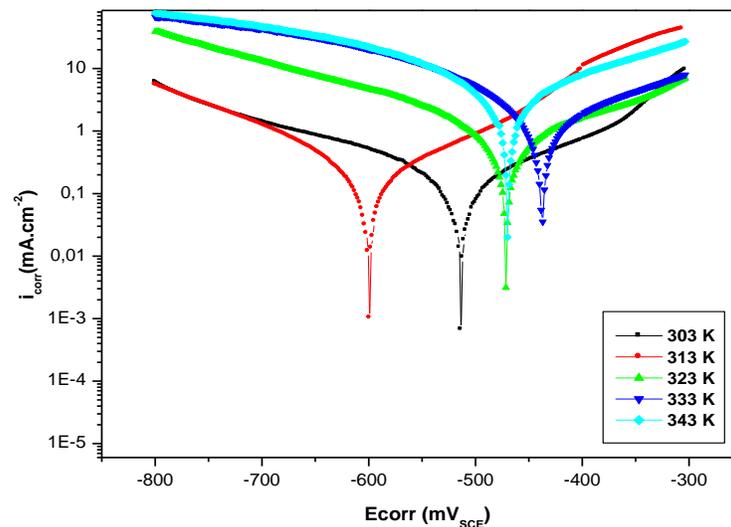
Figure 10: Potentiodynamic polarization curves for steel in 1M HCl at various temperatures for concentration 2.4 g/L the E oil inhibitor.
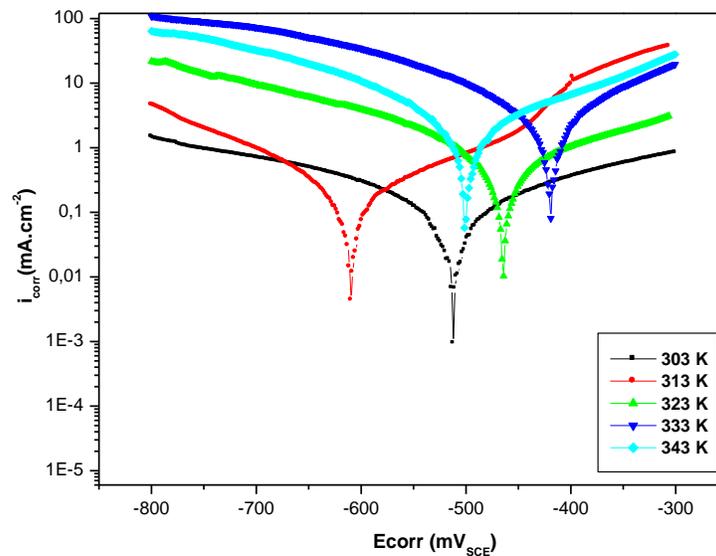
Figure 11: Potentiodynamic polarization curves for steel in 1M HCl at various temperatures for concentration 3 g/L the E oil inhibitor.

It is clear from Table 5, that corrosion current density increased with temperature in the absence (1M HCl) and in the presence of different concentrations of Carum.C E oil. It was found that the corrosion current density of carbon steel, in free and inhibited acid solutions increase with a rise in temperature. However, the inhibition efficiency decreases with rise in temperature. These findings confirm that Carum.C E oil is an effective inhibitor in the range of temperature studied.

Table 4: Polarization parameters and corresponding inhibition efficiency for the corrosion of the C38 in 1M HCl without and with addition of various concentrations of Carum.C E oil at different temperatures.

Inhibitors (g/L)	Temp (K)	Ecorr (mV$_{SCE}$)	Icorr (µA.cm^{-2})	IE (%)	θ
Blank	303	-451.63	144.71	-	-
	313	-543.01	81.56	-	-
	323	-426.14	415.23	-	-
	333	-417.30	697.38	-	-
	343	-423.67	689.49	-	-
0.6	303	-474.48	32.14	78	**0.78**
	313	-563.76	32.35	60	**0.60**
	323	-446.39	210.28	49	**0.49**
	333	-445.52	424.37	39	**0.39**
	343	-419.20	454.00	39	**0.39**
1.2	303	-477.52	26.93	81	**0.81**
	313	-591.06	30.39	63	**0.63**
	323	-438.35	182.84	45	**0.45**
	333	-435.64	400.95	43	**0.43**
	343	-433.89	415.57	40	**0.40**
1.8	303	-498.18	24.66	83	**0.83**
	313	-604.44	28.79	65	**0.65**
	323	-441.06	168.56	54	**0.54**
	333	-435.64	388.95	44	**0.44**
	343	-448.22	399.91	42	**0.42**
2.4	303	-426.90	22.69	84	**0.84**
	313	-599.10	16.20	80	**0.80**
	323	-461.16	147.94	65	**0.65**
	333	-437.59	333.00	52	**0.52**
	343	-431.18	351.75	49	**0.49**
3	303	-512.33	12.09	92	**0.92**
	313	-609.85	15.61	81	**0.81**
	323	-465.26	81.06	69	**0.69**
	333	-477.54	238.80	66	**0.66**
	343	-447.27	336.00	51	**0.51**

The kinetic parameters are given in Table 5. The apparent activation energy, Ea of the corrosion reaction was determined using Arrhenius plots. The Arrhenius equation could be written as:

$$I_{corr} = A \exp\left(\frac{-Ea}{RT}\right) \qquad (8)$$

where I_{cor} is the current density , Ea is the apparent activation energy of the carbon steel dissolution, R is the molar gas constant, T is the absolute temperature, and A the Arrhenius pre-exponential factor.

The apparent activation energy (Ea) of the corrosion reaction in presence and absence of the inhibitor could be determined by plotting ln (I_{corr}) versus 1/T which gives a straight line (Fig. 12) with a slope permitting the determination of Ea. Fig. 12 shows the Arrhenius plots in absence and presence of various concentrations of Carum.C E oil. The corresponding values of E_a are given in Table bellow (Table 6) and indicate that values of Ea obtained in solutions containing Carum.C E oil are lower than those in the inhibitor free acid solutions. The increase in Ea with HE concentration as shown in Table 4 is typical of physisorption mechanism [52].
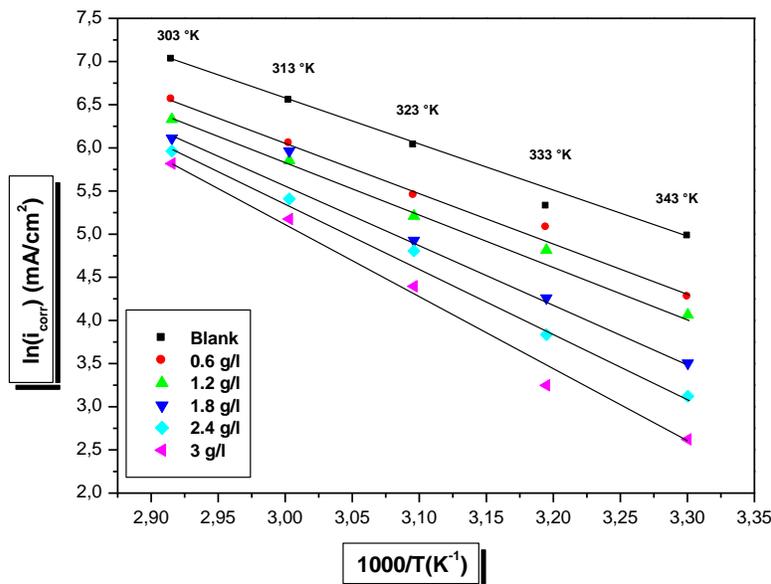
Figure 12 : Arrhenius plots for the corrosion current density of C_{38} in 1M HCl without and with concentrations of Carum.C E oil at different temperatures

An alternative formulation of Arrhenius equation (Eyring transition state equation) is [53]:

$$\text{Icorr} = \frac{RT}{N_A h} \exp\left(\frac{\Delta S^\circ}{R}\right) \exp\left(-\frac{\Delta H^\circ}{RT}\right) \qquad (9)$$

where h is Planck's constant, N_A Avogadro's number, R the universal gas constant, ΔH° the enthalpy of the activation and ΔS^* is the entropy of activation. Fig.13 shows a plot of ln (icorr/T) against 1/T. Straight lines are obtained with a slope of $\left(\frac{-\Delta H^\circ}{R}\right)$ and an intercept of $\left(\ln\left(\frac{R}{N_A h}\right) + \left(\frac{\Delta S^\circ}{R}\right)\right)$ from which the values of ΔH° and ΔS° are calculated and listed in Table 5 (delta H and delta S). The positive signs of ΔH° in Table (5) reflect the endothermic nature of steel dissolution process suggesting that the dissolution of steel is slow [54]. The values of entropy of activation in the presence and absence of Carum.C E oil are positive and increase with temperatures, this implies that an increase in disorder.

Table 5: Activation parameters, Ea, ΔH°_a, ΔS°_a, of the dissolution of C38 in 1 M HCl in the absence and presence of various concentrations of Carum.C E oil

	ΔH°_a (kJ.mol^{-1})	E_a (kJ.mol^{-1})	ΔS°_a (J.mol^{-1}·K^{-1})
HCl (1M)	73.04	45.94	69.76
Concentration (g/L)	E.O		
0.6	79.98	48.02	85.04
1.2	81.14	48.18	87.32
1.8	87.17	59.93	103.33
2.4	85.57	62.82	95.05
3	95.35	71.90	120.84
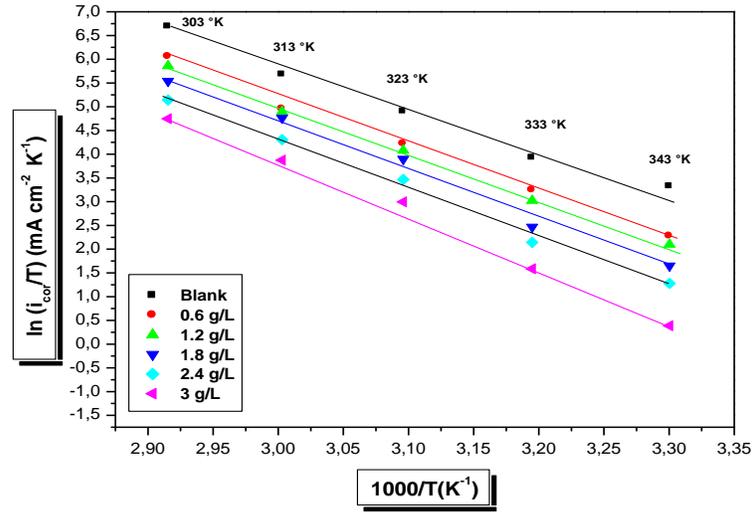
Figure 13: Arrhenius plots of corrosion ln (I_{corr}/T) vs. 1/T for carbon steel in 1M HCl solution in the absence and presence of Carum.C E oil

3.6. Adsorption isotherm:

The mechanism of the interaction between inhibitor and the electrode surface can be explained using adsorption isotherms. Several adsorption isotherms were tested and the Langmuir adsorption isotherm was found to provide best description of the adsorption behavior of the investigated inhibitor (Fig 14), Langmuir adsorption isotherms were obtained according to the following equation:

$$\frac{C_{inh}}{\Theta} = \frac{1}{K_{ads}} + C_{inh} \qquad (10)$$

Where C_{inh} is the concentration of inhibitor, K_{ads} the adsorptive equilibrium constant, θ is the fraction of the surface covered calculated as follows θ = IE(%)/100
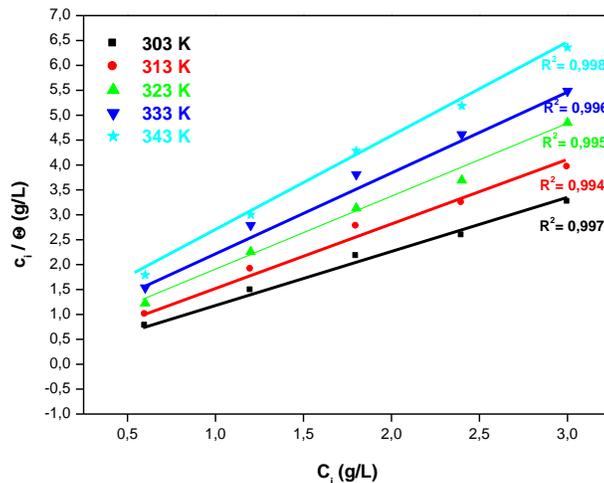
Figure 14: Plots of Langmuir adsorption isotherm of Carum.C E oil on the C38 surface at different temperatures

J. Mater. Environ. Sci. 7 (9) (2016) 3162-3178
ISSN : 2028-2508
CODEN: JMESCN

EL Hattabi et al.

The values of regression coefficients (R^2) confirmed the validity of this approach. Though the linearity of the Langmuir plot (Fig. 14) may be taken to suggest that the adsorption of inhibitor follows the Langmuir isotherm, the considerable deviation of the slope from unity indicated that the isotherm could not be strictly applied. The deviation of the slope could also be interpreted due to the changes in adsorption heat with increasing surface coverage which has also been ignored in the derivation of Langmuir isotherm [55]. The experimental data have been then fitted into the modified form of Langmuir isotherm known as El-Awady isotherm which can appropriately represent the adsorption behavior of the inhibitor onto the iron surface. El-Awady isotherm is given by [56]:

$$\log \left(\frac{\theta}{1-\theta}\right) = \log K + y \log C_{inh} \quad (11)$$

Where, C_{inh} is molar concentration of inhibitor in the bulk solution, θ is the degree of surface coverage, K is the equilibrium constant of adsorption process; $K_{ads} = K^{1/y}$ and y is number of inhibitor molecules occupying one active site. Value of 1/y less than unity implies the formation of multilayer of the inhibitor on the metal surface, while the value of 1/y greater than unity means that a given inhibitor occupy more than one active site [57-60] Curve fitting of the data to the thermodynamic/kinetic model (El-Awady) is shown in Figure 15. The plot gives straight lines which show that the experimental data fits the isotherm. The values of K_{ads}, 1/y and R^2 calculated from the El-Awady isotherm model is listed in Table 6.
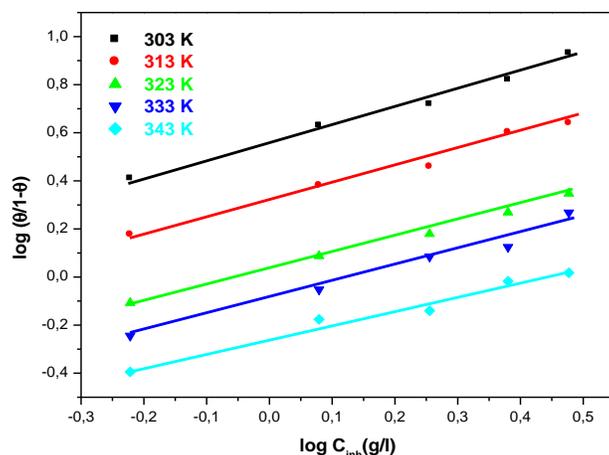
Figure 15: El-Awady's adsorption isotherm model for carbon steel in 1M HCl medium

Table 6: Variations of the absorption coefficient of Carum.C E oil according to different temperatures for C38 in 1M HCl solution

Temperature (K)	K_{ads}	1/y	R^2
303	2.20017	1.4000504	0.99434
313	1.61481	1.49080175	0.9933
323	1.05082	1.56978478	0.99834
333	0.86765	1.43781452	0.98969
343	0.64516	1.71895144	0.98756

The values of K_{ads} decreased in this study with the increase in the temperature (Table 6) indicating that the binding power of the inhibitor to the metal surface decreases with the increasing of temperature and that adsorption of *Carum Carvi* E oil on the carbone steel surface was unfavorable at higher temperature. Such

behavior can be interpreted on the basis that an increase in temperature comes from the desorption of some molecules of the E oil from the metal surface.

Conclusions

The main results of the current work are summed up as follows:

➢ *Carum Carvi* E oil is good inhibitor for the corrosion of carbon steel in 1M HCl medium and Polarization study showed that the oil was cathodic type inhibitor.

➢ The inhibition efficiency of the *Carum Carvi* E oil increased with the concentration and reached 92 % at $3g.L^{-1}$

➢ The inhibition efficiency decreased with increasing temperature and their addition led to an increase of the activation corrosion energy.

➢ A good agreement is obtained for the inhibition efficiency determined by weight loss, polarization curves and electrochemical impedance spectroscopy methods.

➢ The corrosion process was inhibited by the adsorption of *Carum Carvi* E oil on the carbon steel surface fits Langmuir isotherm followed by El Awady adsorption model.

References

1. Garcia ArriagaV., Alvarez R.J., Amaya M., *Corros. Sci.* 52 (2010) 2268.
2. Sykes J.M., *Brit. Corros. J.* 25 (1990) 175.
3. Lalitha A., Ramesh S., Rajeswari S., *Electrochim. Acta.* 51 (2005) 47.
4. Bentiss F., Bouanis M., Mernari B., Traisnel M., Vezin H., Lagrenee M., *Appl. Surf. Sci.* 253 (2007) 3696.
5. Bentiss F., Outirite M., Traisnel M., Vezin H., Lagrenée M., Hammouti B., Al-Deyab A.A., Jama C., *Int. J. Electrochem. Sci.* 7 (2012) 1699.
6. Elachauri M., Hajji M.S., Kertit S., Salem E.M., Coudert R., *Corros. Sci.* 37 (1995) 381.
7. Galai M., El Gouri M., Dagdag O., El Kacimi Y., Elharfi A., Ebn Touhami M. *J. Mater. Environ. Sci*. 7 (5) (2016) 1562-1575.
8. Lagrenée M., Mernari B., Bouanis M., Taisnel M., Bentiss F., *Corros. Sci.* 44 (2002) 573.
9. Ahamad I., Prasad R., Quraishi M.A., *Corros. Sci.* 52 (2010) 1472.
10. Chauhan L.R., Gunasekaran G., *Corros. Sci.* 49 (2007)1143.
11. Manssouri M., El Ouadi Y., Znini M., Costa J., Bouyanzer A., Desjobert JM., Majidi L. *J Mater. Environ. Sci. 6 (3) (2015) 631-646*
12. Singh A.K., Quraishi M.A., *Corros. Sci.* 52 (2010) 152.
13. Satapathy A.K., Gunasekaran G., Sahoo S.C., Amit K., Rodrigues P.V., *Corros. Sci.* 51 (2009) 2848.
14. Sethuraman M.G., AishwaryaV., Kamal C., *Arabe. J. Chem.* 10 (2013) 1016.
15. Hamdy A., El-Gendy Egypte N.Sh., *J. Essence.* 22 (2013) 17.
16. Behpoura M., Ghoreishia S.M., Khayatkashania M., Soltanib N., *Mater. Chem. Phys.* 131 (2012) 621.
17. El-Ashry E.H., El-Nemir A., Esawy S.A., Ragab S., *Electrochim. Acta.* 51 (2006) 3957.
18. Sethuran M.G., Raja P.B., *Pigm. Resin. Technol.* 34 (2005) 327.
19. El Bribri A., Tabyaoui M., Tabyaoui B., El Attari H., Bentiss F., *Mater. Chem. Phys.* 141 (2013) 240.
20. Bouyanzer A., Hammouti B., Majidi L., *Mater. Lett.* 60 (2006a) 2840.
21. Faska Z., Majidi L., Fihi R., Bouyanzer A., Hamouti B., *Pigm. Resin. Technol.* 36 (2007)293.
22. Hmamou D. B., Salghi R., Zarrouk A., Hammouti B., Al-Deyab S. S., Bazzi Lh., Zarrouk H., Chakir A., Bammou L., *Int. J. Electrochem. Sci.* 7 (2012) 2361.
23. Bouyanzer A., Majidi L., Hammouti B., *Bull. Electrochem.* 22 (2006b) 321.
24. Rekkab S., Zarrok H., Salghi R., Zarrouk A., Bazzi Lh., Hammouti B., Kabouche Z., Touzani R., Zougagh M. *J. Mater. Environ. Sci. 3 (4) (2012) 613-627*
25. Aziate G., El Yadini A., Saufi H., Almaofari A., Benhmama A., Harhar H., Gharby S., El Hajjaji S. *J. Mater. Environ. Sci*.6 (7) (2015) 1
26. Chaieb E., Bouyanzer A., Hammouti B., Benkaddour M., Berrabah M., *Trans. SAES. Technol.* 39 (2004) 58.

27. El Ouariachi E., Paolini J., Bouklah M., Elidrissi A., Bouyanzer A., Hammouti B., Desjobert J.M., Costa J., *Acta. Metall. Sin.* 23 (2010) 13.
28. Ouachikh O., Bouyanzer A., Bouklah M., Desjobert J.M., Costa J., Hammouti B., Majidi L., *Surf. Rev. Lett.* 16 (2009) 49.
29. Benabdellah M., Benkaddour M., Hammouti B., Bendahou M., Aouiti A., *Appl. Surf. Sci.* 252 (2006) 6212.
30. Bouyanzer A., Hammouti B., *Pigm. Resin. Technol.* 33 (2004) 287.
31. Zerga B., Sfaira M., Rais Z., Ebn Touhami M., Taleb M., Hammouti B., Imelouane B., Elbachiri A., *Mater. Technol.* 97 (2009) 297.
32. Faska Z., Majidi L., Fihi R., Bouyanzer A., Hamouti B., *Pigm. Resin. Technol.* 36 (2007) 293.
33. Chaieb E., Bouyanzer A., Hammouti B., Benkaddour M., *Appl. Surf. Sci.* 246 (2005) 199.
34. Faska Z., Bellioua A., Bouklah M., Majidi L., Fihi R., Bouyanzer A., Hammouti B., *Monatsh. Chem.* 139 (2008) 1417.
35. Chaieb E., Bouyanzer A., Hammouti B., Berrabah M., *Acta. Phys. Chim. Sin.* 25 (2009) 1254.
36. Clevenger J.F., *J. Pharm. Sci.* 17 (1928) 345.
37. Wiley Registry of Mass Spectral Data, with NIST Spectral Data CD Rom, 7th ed.; John Wiley & Sons: New York, NY, USA, 1998.
38. Lemmon E.W., McLinden M.O., Friend D.G., Linstrom P.J., Mallard W. G., *NIST Chemistry WebBook*. 69 (2005).
39. Davies N.W., *J. Chromatogr.* 503 (1990) 1.
40. Sparkman David O., *J. Am. Soc. Mass Spectrom.* 8 (1997) 671.
41. Li X.H., Deng S.D., Mu G.N., Fu H., Yang F.Z., *Corros. Sci.* 50 (2008) 420.
42. Li X.H., Deng S.D., Fu H., Mu G.N., *Corros. Sci.* 50 (2008) 2635.
43. Vracar L.M., Drazic D.M., *Corros. Sci.* 44 (2002) 1669.
44. Stern M., Geary A.L., *J. Electrochem. Soc.* 104 (1957) 56.
45. Bentiss F., Traisnel M., Chaibi N., Mernari B., Vezin H., Lagrenée M., *Corros. Sci.* 44 (2002) 2271.
46. Tsuru T., Haruyama S., Gijutsu B., *J. Jpn. Soc. Corros.* 27 (1978) 573.
47. Schweinsberg D.P., Ashworth V., *Corros. Sci.* 28 (1988) 539.
48. Musa A.Y., Jalgham R.T.T., Mohamad A.B., *Corros. Sci.* 56 (2012) 176.
49. Aramaki K., Hagiwara M., Nishihara H., *Corros. Sci.* 5 (1987) 487.
50. El-Etre A.Y., Abdallah M., El-Tantawy Z.E., *Corros. Sci.* 47 (2005) 385.
51. Obot I.B., Obi-Egbedi N.O., Eseola A.O., *Ind. Eng. Chem. Res.* 50 (2011) 2098.
52. Li X.H., Deng S.D., Fu H., Mu G.N., *Corros. Sci.* 51 (2009) 620.
53. Guan N.M., Xueming L., Fei L., *Mater. Chem. Phys.* 86 (2004) 59.
54. Olivares O., Likhanova N.V., Gomez B., Navarrete J., Llanos-serran M.E., Arce E., Hallen J.M., *App. Surf. Sci.* 252 (2006) 2894.
55. Oguzie E.E., Okolue B.N., Ebenso E.E., Onuoha G.N., Onuchukwu A.I., *Mater. Chem. Phys.* 87 (2004) 401.
56. El-Awady A.A., Abd-El-Nabey B.A., Aziz S.G., *J. Electrochem. Soc.*139 (1992) 2154.
57. Singh. A.K., Shukla S.K., Singh M., Quraishi M.A., *Mater. Chem. Phys.* 129(1) (2011) 76.
58. Ibot I.B., Obi-Egbedi N.O., Umoren S.A., *Int. J. Electrochem. Sci.* 4 (2009) 863.
59. Singh A.K., Quraishi M.A., *Corros. Sci.* 53 (2011) 1288.
60. El Ouasif L., Merimi I., Zarrok H., El ghoul M., Achour R., Guenbour M., Oudda H., El-Hajjaji F., Hammouti B. *J. Mater. Environ. Sci.* 7 (8) (2016) 2718-2730.

(2016) ; http://www.jmaterenvironsci.com/